Molecular and Cellular Neuroscience 128 (2024) 103919

Contents lists available at ScienceDirect

Molecular and Cellular Neuroscience

journal homepage: www.elsevier.com/locate/ymcne

Alpha-synuclein pathology is associated with astrocyte senescence in a midbrain organoid model of familial Parkinson's disease

Mudiwa N. Muwanigwa [a,1,2], Jennifer Modamio-Chamarro [a,1,3], Paul M.A. Antony [b], Gemma Gomez-Giro [a], Rejko Krüger [c], Silvia Bolognin [a,4,5], Jens C. Schwamborn [a,*,5]

[a] Developmental and Cellular Biology, Luxembourg Centre for Systems Biomedicine, University of Luxembourg, L-4367 Belvaux, Luxembourg
[b] Bioimaging Platform, Luxembourg Centre for Systems Biomedicine, University of Luxembourg, L-4367 Belvaux, Luxembourg
[c] Translational Neuroscience, Luxembourg Centre for Systems Biomedicine, University of Luxembourg, L-4367 Belvaux, Luxembourg

ARTICLE INFO

Keywords:
α-Synuclein
Astrosenescence
Midbrain organoids

ABSTRACT

Parkinson's disease (PD) is a complex, progressive neurodegenerative disease characterized by the loss of dopaminergic neurons in the substantia nigra pars compacta in the midbrain. Despite extensive research efforts, the molecular and cellular changes that precede neurodegeneration in PD are poorly understood. To address this, here we describe the use of patient specific human midbrain organoids harboring the *SNCA* triplication to investigate mechanisms underlying dopaminergic degeneration. Our midbrain organoid model recapitulates key pathological hallmarks of PD, including the aggregation of α-synuclein and the progressive loss of dopaminergic neurons. We found that these pathological hallmarks are associated with an increase in senescence associated cellular phenotypes in astrocytes including nuclear lamina defects, the presence of senescence associated heterochromatin foci, and the upregulation of cell cycle arrest genes. These results suggest a role of pathological α-synuclein in inducing astrosenescence which may, in turn, increase the vulnerability of dopaminergic neurons to degeneration.

1. Introduction

As the most common movement disorder and second most common neurodegenerative disease, Parkinson's disease (PD) poses a significant healthcare and societal challenge. Pathologically, PD is characterized by the selective loss of dopaminergic neurons in the substantia nigra pars compacta of the midbrain. Moreover, PD is also characterized by the widespread presence of cytoplasmic and neuritic protein inclusions abundant in α-synuclein, known as Lewy bodies and Lewy neurites respectively (Spillantini et al., 1997). α-Synuclein is a small 14 kDa protein encoded by the *SNCA* gene. While its structure is still debated, the general consensus at present is that it exists in a dynamic equilibrium between a cytosolic soluble, intrinsically disordered monomeric form and a lipid-bound α-helical state (Eliezer et al., 2001; Ulmer and Bax, 2005; Waudby et al., 2013; Weinreb et al., 1996). Functionally, α-synuclein has been implicated in playing a role in synaptic function and neurotransmitter release due to its presence in presynaptic terminals and due to the observation that α-synuclein directly interacts with the SNARE-complex through binding with synaptobrevin 2 (Burré et al., 2010; Fortin et al., 2005). Other functions have also been proposed including antiapoptotic activity (Jin et al., 2011; Li and Lee, 2005) and stabilization of the electron transport chain in mitochondria (Bobela et al., 2015). Furthermore, there is an emerging interest in α-synuclein's role in the nucleus (Koss et al., 2022). For example, Schaser et al.

* Corresponding author at: Luxembourg Center for Systems Biomedicine (LCSB), Campus Belval – House of Biomedicine 2, 6, Avenue du Swing, L-4367 Belvaux, Luxembourg.
E-mail address: jens.schwamborn@uni.lu (J.C. Schwamborn).
[1] These authors contributed equally.
[2] Present address: UK Dementia Research Institute at UCL, UCL Cruciform Building, 90 Gower Street, WC1E 6BT London, United Kingdom.
[3] Present address: Institute for Tissue Engineering and Regenerative Medicine, Helmholtz Zentrum München, Ingolstädter Landstraße 1, 85764 Oberschleißheim, Germany.
[4] Present address: Department of Cell Biology-Inspired Tissue Engineering, MERLN Institute for Technology-Inspired Regenerative Medicine, Maastricht University, Maastricht, the Netherlands.
[5] Co-last authors.

https://doi.org/10.1016/j.mcn.2024.103919
Received 30 August 2023; Received in revised form 26 January 2024; Accepted 27 January 2024
Available online 1 February 2024

recently showed that α-synuclein can bind to DNA and modulate the repair of double strand breaks (Schaser et al., 2019). α-synuclein has also been implicated in interacting with Ras-related nuclear protein, which transports RNA and proteins through the nuclear pore complex, thus suggesting that α-synuclein may play some role in nucleocytoplasmic transport (Chen et al., 2020). Despite there being some evidence towards these proposed functions, α-synuclein's physiological role remains unclear.

Point mutations, duplications and triplications of the *SNCA* gene have been shown to cause early onset forms of PD, with an autosomal dominant pattern of inheritance (Singleton et al., 2003; Polymeropoulos et al., 1997; Krüger et al., 1998; Appel-Cresswell et al., 2013; Fujioka et al., 2014; Hoffman-Zacharska et al., 2013; Kiely et al., 2013; Pasanen et al., 2014; Zarranz et al., 2004). Moreover, these mutations lead to the abnormal aggregation of α-synuclein and the increased presence of Lewy pathology (Lashuel et al., 2002; Miller et al., 2004). Pathological α-synuclein has been associated with synaptic dysfunction, mitochondrial dysfunction, increased oxidative stress, perturbation of protein degradation systems, and nuclear dysfunction (Malkus et al., 2009; Choi et al., 2018; Volpicelli-Daley et al., 2011; Geertsma et al., 2022). However, how pathological forms of α-synuclein mediate this dysfunction is not well understood.

Due to limitations in currently used model systems, understanding the temporal mechanisms that underlie α-synuclein pathology in PD remains a pertinent challenge. Rodent models that have predominantly been used in the study of PD often do not capture some of the key characteristic hallmarks observed in PD (Potashkin et al., 2010). The development of stem cell derived human midbrain organoids (hMO) is a profound milestone in PD research as they recapitulate key physiological and functional aspects of the human midbrain (Smits and Schwamborn, 2020; Galet et al., 2020). These self-organizing three-dimensional tissues contain an abundance of dopaminergic neurons. In addition, they contain glial cells, show electrochemical functionality, and dopamine release (Monzel et al., 2017; Jo et al., 2016). We, and others, have described robust protocols for the development of midbrain specific organoids from induced pluripotent stem cells (iPSC) (Monzel et al., 2017; Jo et al., 2016; Nickels et al., 2020). Importantly, these organoids have been used in the modeling of various genetic forms of PD, including forms associated with LRRK2, PINK1 and DJ1 (Smits et al., 2019; Jarazo et al., 2022; Kim et al., 2019; Ahfeldt et al., 2020).

Here, we generate hMO from patient specific iPSC lines harboring the *SNCA* triplication, along with healthy age-sex matched controls and compare them until 90 days of organoid maturation. Our model recapitulates key hallmarks of PD, including the aggregation of α-synuclein and the progressive decline of dopaminergic neurons. Interestingly, we found that these pathological hallmarks were associated with an increase in senescence associated phenotypes specifically in astrocytes including nuclear lamina defects, the presence of senescence associated heterochromatin foci and the upregulation of cell cycle arrest pathways. Our results suggest that pathological α-synuclein contributes to inducing senescence at early stages of PD, increasing the vulnerability of dopaminergic neurons to degeneration.

2. Materials and methods

2.1. iPSC, NESC and organoid culture

The sources of the five induced pluripotent stem cell lines (iPSC) used in this study are detailed in Supplementary Table 1. IPSC were cultured in Essential 8 medium (ThermoFisher, cat no. A1517001) with 1 % Penicillin/Streptomycin (Invitrogen, cat no. 15140122) in Matrigel-coated plates (Corning, cat no. 354277). Passaging was performed with Accutase (Sigma, cat no. A6964) every 3–4 days. Following passaging, cells were cultured in Essential 8 medium supplemented with 10 μM ROCK inhibitor Y-27632 (Merck Millipore, cat no. 688000) for 6–24 h after seeding. The iPSC were characterized for pluripotency markers (Supplementary Fig. 1).

Neuroepithelial stem cells (NESC) were derived from iPSC as previously described (Reinhardt et al., 2013). NESC were maintained in Geltrex-coated plates and cultured in freshly supplemented N2B27 as described previously (Monzel et al., 2017). To obtain a homogeneous population of NESC, the cells were passaged at least five times before performing an immunofluorescence staining to confirm neural stem cell identity (Supplementary Fig. 2).

Following quality assessment of the NESC by immunostaining, midbrain organoids (hMO) were generated as previously detailed (Monzel et al., 2017), with slight modifications. 9000 NESC were plated in each well of an ultra-low attachment 96 well round bottomed plate (Corning, cat no. 7007) and cultured in maintenance medium for 8 days. After the 8 days, the colonies were embedded in 25 μl Geltrex (Invitrogen, cat no. A1413302) and transferred to 24 well ultra-low attachment plates kept at 37 °C, 5 % CO_2 under dynamic conditions (80 rpm) for up to 90 days or were left unembedded in 96-well ultralow adhesion plates (round bottom, Corning, cat no. 7007) (Zagare et al., 2021).

2.2. Western blot

For Western blotting, six non-embedded organoids were lysed using RIPA buffer (Abcam, cat no. ab156034) with cOmplete™ Protease Inhibitor Cocktail (Roche, cat no. 11697498001) for 20 min on ice. In order to disrupt DNA, lysates were sonicated for 10 cycles (30 s on/30 s off) using the Bioruptor Pico (Diagenode). Samples were then centrifuged at 4 °C for 20 min at 14,000 g. The protein concentration for each sample was determined using the Pierce™ BCA Protein Assay Kit (ThermoFisher, cat no. 23225). Samples were adjusted to the same concentration by appropriate dilution with RIPA buffer and boiled at 95 °C for 5 min in denaturating loading buffer. 20 μg of protein was loaded per sample for every Western blot. Protein separation was achieved using SDS polyacrylamide gel electrophoresis (Bolt™ 4–12 % Bis-Tris Plus Gel, ThermoFisher) and transferred onto a PVDF membrane using iBlot™ 2 Gel Transfer Device (ThermoFisher). For α-synuclein and pS129 α-synuclein Western blots, membranes were then fixed in 0.4 % paraformaldehyde (PFA) in PBS for 30 min at room temperature (RT), and then washed twice with PBS for 5 min each wash. Following PVDF transfer or fixation, membranes were blocked for 1 h at RT in 5 % skimmed milk powder and 0.2 % Tween in PBS before incubating overnight at 4 °C with the primary antibodies prepared in 5 % BSA and 0.02 % Tween (see Supplementary Table 2 for list of antibodies used). Membranes were then washed three times for 5 min with 0.02 % Tween in PBS and incubated with DyLight™ secondary antibodies at a dilution of 1:10,000 (anti-rabbit IgG (H + L) 800, Cell Signaling, cat no. 5151P or anti-mouse IgG (H + L) 680, Cell Signaling, cat no. 5470P). Membranes were scanned in the Odyssey® Fc 2800 Imaging System and exposure time was 2 min for all the acquisitions. All conditions were consistently kept the same for all the Western blots at every time point. Western blots were analyzed using ImageJ software. Figures showing Western blots are cropped to display only the cell lines relevant to this study and the original uncropped Western blots can be found in Supplementary original blots.

2.3. Time course Western blot

For the time course of α-synuclein (Fig. 2B), pS129-α-synuclein (Fig. 3B) and TH (Fig. 4D), Western blot analysis was performed as described in detail in the previous section. To ensure robust comparison, the exact same conditions were maintained for each Western blot - Six pooled organoids per line for each batch; 20 μg of protein loaded for SDS gel electrophoresis; same order of sample loading, same period of blocking, primary and secondary incubation; same antibody concentration; and same exposition time of 2 min for membrane reveal using the same instrument (Odyssey Imaging System). Following protein quantification in ImageJ, relative expression levels of the proteins were determined by dividing the intensity of the marker of interest with the

intensity of ß-actin. These values were then used to generate the time course graph. Mean data from three independently derived organoid batches was plotted at each time point (15, 30, 50, 70 and 90 days). Data was pooled for the two wild type lines, and for the two 3xSNCA lines. To plot the time course, a smooth line of best fit was fitted over the mean value at each time point for WT and 3xSNCA using the geom_smooth function from the ggplot2 library in R (R Studio version 1.3.1073). The geom_sooth function is a non-parametric regression method used to fit a smooth curve to sparse data points. Statistical significance was calculated at each time point using Mann-Whitney *U* test in R. Statistically significant results were indicated when *p* values were * < 0.05, ** < 0.01 and *** < 0.001.

2.4. Fractionation of soluble and insoluble α-synuclein

12 non-embedded organoids per cell line were collected and incubated in 250 µl of lysis buffer (1 % Triton-X 100 with protease inhibitor and phosphatase inhibitor) for 25 min on ice. Samples were then lysed by pipetting and sonicated for 10 cycles (30 s on, 30 s off). Lysates were transferred to ultracentrifuge tubes (Beckman Coulter Polycarbonate Centrifuge Tubes, cat no. 343776) and spun down at 100,000 *g* for 45 min at 4 °C. The supernatant (i.e., the soluble fraction) was collected and stored at −80 °C or used immediately in Western Blot. The remaining pellet was resuspended in 120 µl of 8 M urea +8 % SDS and allowed to incubate for 15 min, after which the samples were sonicated for 10 cycles (30 s on, 30 s off). The resulting lysate represented the insoluble protein fraction, which was subsequently stored at −80 °C or used in a Western Blot as already described above.

2.5. Dot Blot for α-synuclein

200 µl of media was collected from three individual non-embedded organoids per line, then snap frozen or directly used. Media was thawed on ice and spun down at 300 *g* at 4 °C for 5 min to sediment any cell debris remaining in media. A Dot Blot Minifold I (Whatman; 10,447,900) was used according to manufacturer guidelines. A nitrocellulose membrane (Sigma-Aldrich, cat no. GE10600001) was rehydrated twice with 300ul of PBS per well before sample loading. After sample run (vacuum ON), the membrane was washed with 300 µl of PBS per well. Membrane was retrieved and fixed in 0.04 % PFA in PBS for 30 min at RT, followed by 1 min wash in PBS to remove the PFA. Blocking and antibody incubation were done exactly as previously described in the Western blotting section. Images were acquired with the Odyssey® Fc 2800 Imaging System. Images were analyzed with ImageJ. Relative α-synuclein amount was normalized to the individual organoid diameter.

2.6. Immunofluorescence stainings for iPSC and NESC characterization

Immunofluorescent stainings for iPSCs and NESC were perform as previously described in Gomez-Gomez-Giro et al. (2019) and Monzel et al. (2017) respectively.

2.7. Immunofluorescence staining of organoid sections

Immunofluorescence staining of organoids was carried out using a published protocol with slight modifications (Nickels et al., 2020). Organoids were fixed with 4 % PFA overnight at 4 °C, and then washed with PBS three times for 15 min. Individual organoids (at least three organoids per line for each time point) were embedded in 3 % low-melting point agarose. Using a vibrating blade microtome (Leica VT1000s), the organoids were then sliced into 70 µm sections. The sections were permeabilized and blocked with blocking buffer (5 % normal goat serum, 2.5 % BSA, and 0.1 % sodium azide) containing 0.5 % Triton X-100. Sections were incubated for 48 h at 4 °C on an orbital shaker with primary antibodies (see Supplementary Table 2) in blocking buffer containing 0.1 % Triton X-100. Secondary antibody incubation and mounting of sections was performed as previously described (Nickels et al., 2020).

2.8. Image acquisition

For high-content image analysis, at least three sections from three organoids of each line in three independent organoid batches were acquired using the Yokogawa CV8000 high content screening microscope with a 20× objective. For quantitative analysis of laminB1 at 40×, a confocal laser scanning microscope (Zeiss LSM710) was used. Three randomly selected fields per organoid section were acquired in at least three organoids per line for three independent organoid batches, keeping the same acquisition settings.

Qualitative images were acquired using a confocal laser scanning microscope (Zeiss LSM 710) with either a 20×, 40× or 60× objective.

2.9. Dopamine extracellular release

Dopamine ELISA (Immusmol BA-E-5300, cat no. BA-E-5300R) was performed for the quantitative determination of dopamine secreted by midbrain organoids at 30 days and 70 days from 3 independent organoid batches. 180 µl of media was collected per organoid (three organoids per line) and 20 µl HCl buffer (0.01 M HCl, 4 mM Na2O5S2, and 1 mM EDTA) was added to each sample. Samples were then frozen in liquid nitrogen and stored at −80 °C until the day of the analysis. The ELISA was performed according to the manufacturer's instructions.

2.10. Quantitative PCR

For total RNA extraction, RNeasy Mini Kit (Qiagen, cat no. 74106) was used following the manufacturer's instructions. For cDNA synthesis High-Capacity RNA-to-cDNA™ Kit (Thermo Fisher Scientific, cat no. 4387406) was used following manufacturer's instructions. Maxima SYBR Green qPCR Master Mix (Thermo Fisher Scientific, cat no. K0221) was used together with the following primers for *CDNK2A*: Forward primer ATCATCAGTCACCGAAGGTC and Reverse primer CTCAAGAGAAGCCAGTAACC and for *ACTIN*: Forward primer TCAAGATCA TTGCTCCTCCTGAG and Reverse primer ACATCTGCTGGAAGGTGGACA. Quantitative PCR was performed in the Aria Mx Real-Time PCR system (Aligent) and AriaMx PC software was used for data extraction and analysis.

2.11. Image processing and analysis

Immunofluorescence 3D images of each organoid section obtained from the Yokogawa or LSM710 were processed and analyzed in Matlab (2020a, Mathworks) using a custom image-analysis algorithm as described previously (Bolognin et al., 2019; Monzel et al., 2020).

2.12. Data processing and statistical analysis

Data plots were generated in GraphPad except for Figs. 2B, 3B and 4D, which were generated in R Studio. Data are presented as mean ± standard deviation. Data was pooled for the two wild type lines, and for the two 3xSNCA lines, and denoted as WT and 3xSNCA respectively in figures. Statistical significance was calculated using Mann-Whitney *U* test in GraphPad or R. Statistically significant results were indicated when *p* values were * < 0.05, ** < 0.01 and *** < 0.001. The number (*N*) of samples, replicates and batches are described in the Figure legends.

2.13. Ethics statement

The use of existing iPSC lines obtained from previous studies was approved by the local ethical committee (Comité National d'Ethique de

Recherche, CNER No 201901/01). Informed consent was obtained from all individuals donating samples to this study prior to the donation using a written form and protocol. Cell lines used in this study are summarized in Supplementary Table 1.

3. Results

3.1. Generation and characterization of human midbrain organoids

To investigate whether we could recapitulate PD relevant pathology in vitro, we generated hMO from two independent iPSC clones derived from a PD patient with the *SNCA* triplication (3xSNCA-1 and 3xSNCA-2) and two sex-age matched healthy control iPSC lines (WT-1 and WT-2) (Supplementary Table 1). An *SNCA* knockout line isogenic to WT-2 (SNCA-KO) was also included for validation of the specificity of α-synuclein antibodies in some assays. All iPSCs were positive for pluripotency markers SOX2, OCT4, TRA-1-81, TRA-1-60, NANOG, and SSEA-4 as assessed by immunocytochemistry (Supplementary Fig. 1). Neuroepithelial stem cells (NESC) were derived from the iPSC lines as previously described (Reinhardt et al., 2013). These neural progenitors are patterned towards a midbrain/hindbrain fate, thus increasing differentiation efficiency towards midbrain cell types. We confirmed the identity of NESCs by immunostaining with SOX2, PAX6 and Nestin (Supplementary Fig. 2).

To generate the hMO, we used our previously published protocol (Monzel et al., 2017). Organoids were either embedded in a Geltrex droplet and maintained under shaking conditions or kept unembedded in 96-well ultra-low attachment plates depending on the downstream assay to be performed (Fig. 1A). We performed a characterization of the WT hMO to ensure that they expressed the relevant cell types of the midbrain. At 15 days of maturation, hMO display regional organization, with the presence of stem cell niches enriched in SOX2+ cells and the presence of tyrosine hydroxylase (TH) positive dopaminergic neurons in the periphery (Fig. 1B, upper panels). At 30 days, there is an abundance of MAP2 positive mature neurons, some of which are dopaminergic neurons (Fig. 1B, third panel). At later time points (>50 days of differentiation) we also observe increased astrogenesis as denoted by increased presence of GFAP+ and S100β + cells (Fig. 1B, lower panel). The hMO show a progressive increase in dopamine release as they mature (Supplementary Fig. 3A). Altogether, the hMO show cellular heterogeneity and the presence of functional dopaminergic neurons.

3.2. 3xSNCA hMO show elevated levels of α-synuclein and α-synuclein related pathological hallmarks

The accumulation and aggregation of α-synuclein is one of the main neuropathological hallmarks of PD. To validate whether this hallmark was recapitulated in our patient specific model, we assessed α-synuclein levels in the organoids. For our analysis, we collectively compared organoids with the *SNCA* triplication (3xSNCA hMO) to the controls (WT hMO) by pooling data from organoids derived from the two 3xSNCA iPSC clones and the two WT lines respectively. Using Western blot, we found significantly higher levels of α-synuclein in the 3xSNCA hMO in comparison to the healthy WT hMO across all assessed time points ranging from 15 to 90 days of organoid culture (Fig. 2A, B). Expression of α-synuclein was confirmed to be largely in neurons, as we observed colocalization of α-synuclein and the neuronal marker MAP2 (Fig. 2C). Furthermore, the specificity of the α-synuclein antibody was confirmed by the lack of signal in the SNCA KO organoids. 3xSNCA hMO also showed higher extracellular release of α-synuclein in the culture medium at Day 30 (Supplementary Fig. 3C, D) and Day 70 (Fig. 2D) as assessed by dot blot.

The phosphorylation of α-synuclein at serine 129 (pS129) has been associated with aggregation and toxicity of the protein and is an important hallmark of α-synuclein pathology formation (Anderson et al., 2006). We therefore assessed the expression of pS129 α-synuclein in our hMO model. We found significantly higher levels of pS129 α-synuclein in the 3xSNCA hMO across all assessed time points in Western blots (Fig. 3A, B). Immunofluorescence staining also confirmed the higher expression of pS129 α-synuclein in the 3xSNCA organoids, specifically in neurons (Fig. 3C). Interestingly, we could also observe the presence of pS129 rich aggregate-like structures in the neuronal cytoplasm and neurites within 3xSNCA hMO which were not observed in WT hMO (Fig. 3D, Supplementary Fig. 4A). These structures could potentially represent the formation of Lewy-body like pathology in the 3xSNCA hMO. Once again, we validated the specificity of the α-synuclein and pS129 α-synuclein antibodies used in the stainings by confirming the absence of signal in the 3xSNCA KO organoid sections (Fig. 3C). Finally, we performed extraction of insoluble α-synuclein, which represents the aggregated form of the protein. Immunoblotting of the insoluble α-synuclein fraction showed significantly higher levels of aggregated α-synuclein in the 3xSNCA hMO at 50 days of organoid maturation (Fig. 3E, F). Our findings show that 3xSNCA hMO can model the accumulation and aggregation of α-synuclein and its phosphorylated form as is observed in PD.

3.3. 3xSNCA hMO show dopaminergic neuron loss

The progressive loss of dopaminergic neurons in the substantia nigra pars compacta is a key neuropathological hallmark of PD. To assess whether we observed this hallmark in our 3xSNCA hMO, we performed an immunofluorescence staining (Fig. 4A), which revealed no difference in the levels of dopaminergic neurons at 30 days, as determined by quantifying the levels of TH+ neurons in the hMO (Fig. 4B, left panel). However, at 70 days, we found significantly less dopaminergic neurons in the 3xSNCA hMO compared to WT (Fig. 4B, right panel), showing a decline in dopaminergic neurons at the later time points in the patient-specific organoids. To further explore this, we assessed the protein levels of the TH enzyme across several time points from 15 to 90 days of organoid maturation using immunoblotting. We observed a tendency towards higher TH levels in the 3xSNCA hMO up until 30 days (Fig. 4C, D). The TH levels subsequently dropped at later time points (after 50 days) in the 3xSNCA hMO compared with the WT hMO, and at 90 days this difference was significant. Thus, we observe a progressive loss of dopaminergic neurons in the patient-specific midbrain organoids.

Dopaminergic neurons produce and release the neurotransmitter dopamine. In the context of PD, the decline of dopaminergic neurons reduces the release of dopamine in the striatum, leading to many of the motor deficits observed in the disease. At 30 days, we found no difference in dopamine release levels in the 3xSNCA and WT hMO (Supplementary Fig. 3B), whereas at 70 days we observed significantly lower levels of extracellular dopamine released by 3xSNCA hMO (Fig. 4E). This observation further reflects the dopaminergic neuron decline observed in the immunostainings and Western blots. Taken together, we see that the 3xSNCA organoids show a progressive loss of dopaminergic neurons.

3.4. Increased 3xSNCA expression is associated with a senescent-like phenotype

Senescence is a cellular state characterized by cell cycle arrest, resistance to apoptosis, nuclear dysfunction and the acquisition of a proinflammatory secretory phenotype (Hernandez-Segura et al., 2018). While senescence has important physiological functions in the body, the accumulation of senescent cells has been shown to be damaging to tissues primarily due to the effects of the senescence associated secretory phenotype (Kumari and Jat, 2021). Senescence has emerged as a relevant mechanism in neurodegenerative diseases such as Alzheimer's and Parkinson's (Kritsilis et al., 2018; Martínez-Cué and Rueda, 2020). Recent studies have suggested that pathological α-synuclein may be an inducer of senescence (Yoon et al., 2022; Verma et al., 2021). Thus, we sought to investigate whether our 3xSNCA hMO model displayed any of

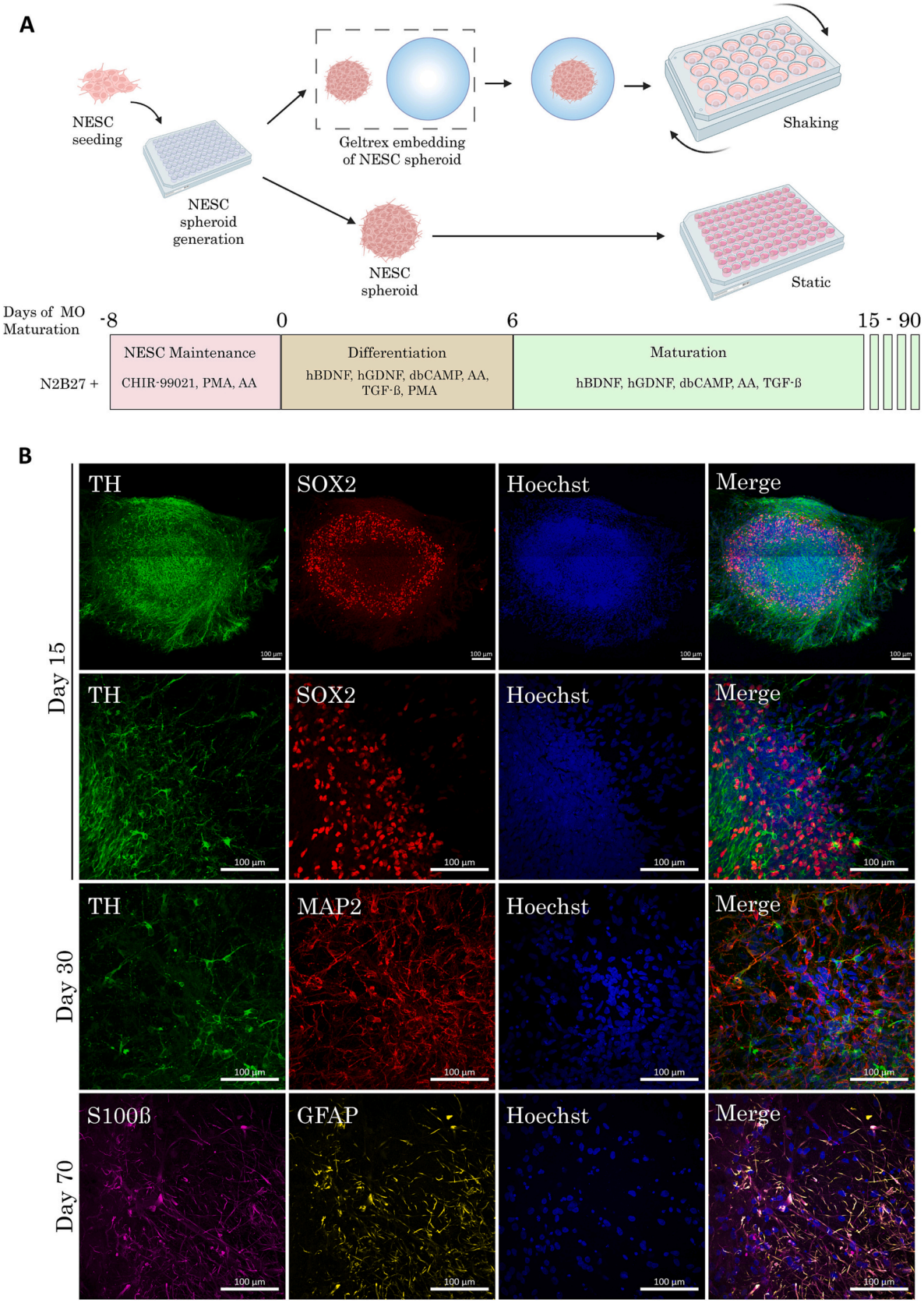

Fig. 1. Recapitulation of human midbrain development in hMO. (A) Schematic overview of the hMO generation protocol. NESC – neuroepithelial stem cell. Created in BioRender. (B) Representative immunostainings of hMO sections at 15 days of organoid maturation, showing the presence of TH+ dopaminergic neurons and SOX2+ neural stem cells (upper panels); 30 days of organoid maturation showing TH+ dopaminergic neurons, some of which colocalize with MAP2, a marker for mature neurons (third panel); and 70 days, showing the presence of S100β + and GFAP+ astrocytes (lower panel). Scale bars = 100 µm. TH – tyrosine hydroxylase. SOX2 – SRY-box2. MAP2 – microtubule associated protein 2. S100β – S100 calcium binding protein B. GFAP – glial fibrillary acidic protein.

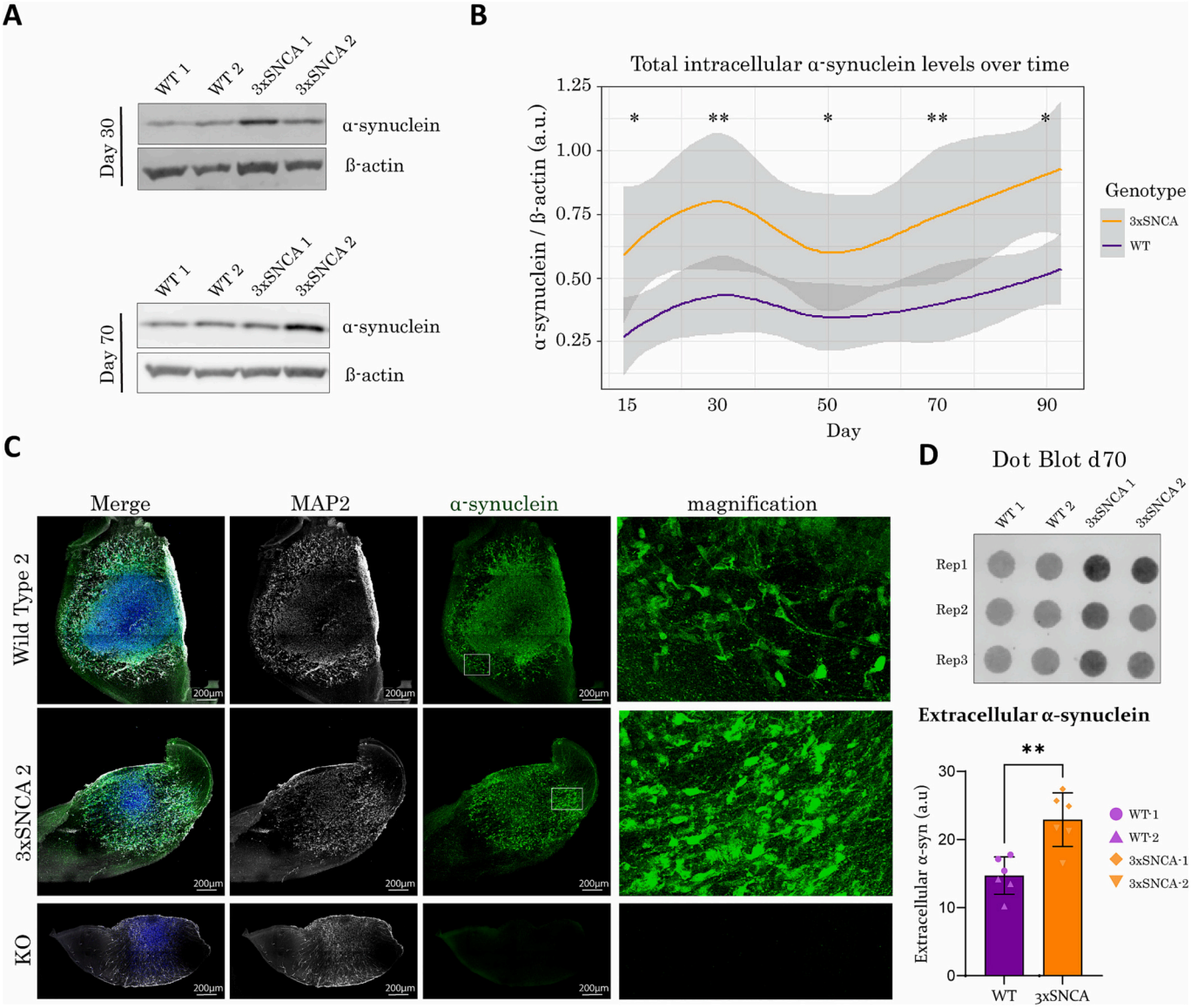

Fig. 2. Increased intracellular and extracellular α-synuclein in 3xSNCA hMO. (A) Representative immunoblots of α-synuclein and β-actin at 30 and 70 days of organoid maturation in WT and 3xSNCA hMO. Western blots are cropped from original images found in Supplementary original blots. (B) Time course of intracellular α-synuclein levels as determined by immunoblots performed at 15, 30, 50, 70 and 90 days of organoid maturation. 3xSNCA hMO show consistently higher levels of α-synuclein across all time points compared to WT hMO. The data represents the summary of three independent hMO batches and is plotted by mutation (WT vs 3xSNCA). Statistical significance by Mann-Whitney *U* test: $*p < 0.05$ and $**p < 0.01$. Extensive description for how the graph was plotted is in materials and methods. (C) Representative images of 30-day old hMO stained with α-synuclein (green) and mature neuron marker MAP2 (white). Specificity of the α-synuclein antibody was confirmed by the absence of staining in the SNCA KO sections. Scale bar = 200 µm. (D) Representative dot blot (upper panel) showing higher levels of extracellular α-synuclein released by 3xSNCA hMO (lower panel) at 70 days. Data represents points represent individual organoids from three independent hMO batches, $N = 2–3$ hMO per line. Data presented as mean ± s.d. Statistical significance by Mann-Whitney U test: $**p < 0.01$. Rep = replicate. Dot blot is cropped from original image found in Supplementary original blots. (For interpretation of the references to color in this figure legend, the reader is referred to the web version of this article.)

the key senescence related hallmarks.

First, we decided to investigate the presence of senescence associated hallmarks specifically in astrocytes. PD patients have been shown to display elevated levels of astrocytes positive for senescent markers (Chinta et al., 2018). Moreover, senescence has been better characterized in astrocytes compared to neurons, due to the postmitotic nature of neuronal cells (Sikora et al., 2021). Initially, we investigated astrocyte levels in the organoids by immunofluorescence staining (Fig. 5A) and strikingly we found higher levels in the 3xSNCA hMO than in the WT hMO (Fig. 5B) as assessed by quantification of GFAP+ cells. Using an automated Matlab image analysis script that can extract morphometric features from images, we analyzed the complexity of the astrocytes as expressed by the number of branches (links) and points of bifurcation (nodes). This revealed more extensive branching in astrocytes in the 3xSNCA organoids, which may be indicative of increased reactivity (Fig. 5C).

Next, we assessed the expression of lamin B1, a nuclear lamina protein that is important in maintaining nuclear integrity (Camps et al., 2015; Butin-Israeli et al., 2015). Loss of lamin B1 is strongly associated with cellular senescence in various cell types, including astrocytes (Freund et al., 2012; Matias et al., 2022). We performed immunostaining of lamin B1 in the organoids (Fig. 5A) and using the Matlab script, we specifically analyzed the expression of laminB1 in astrocyte nuclei. We found a significant reduction in lamin B1 in astrocytes in the 3xSNCA hMO compared to WT hMO at 50 days of maturation (Fig. 5D), which is indicative of senescence. The presence of DNA double strand breaks is

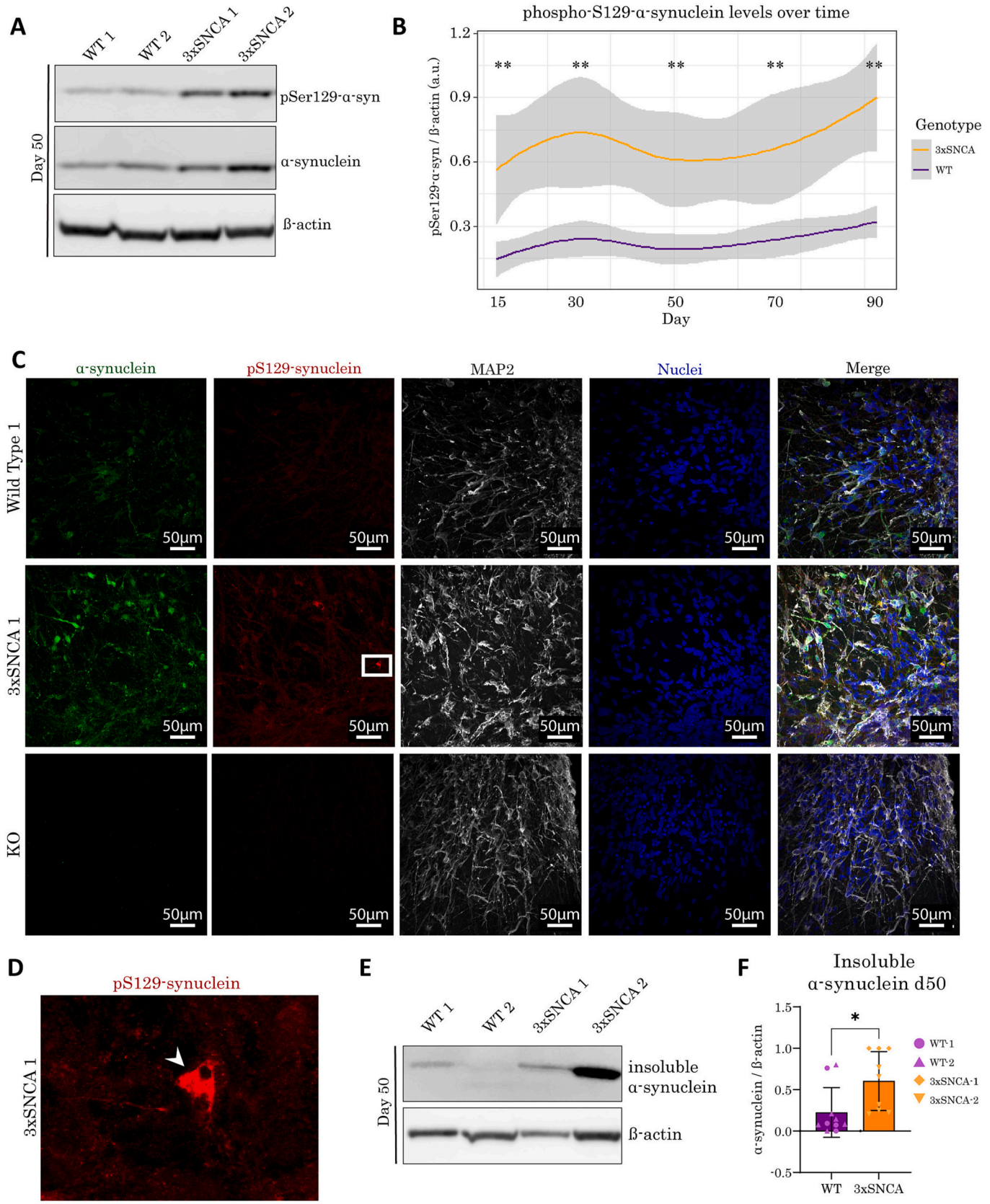

(caption on next page)

Fig. 3. Increased pS129 α-synuclein in 3xSNCA hMO. (A) Representative immunoblots of pS129 α-synuclein, total α-synuclein and β-actin at 50 days of organoid maturation in WT and 3xSNCA hMO. Western blot is cropped from original images found in Supplementary original blots. (B) Time course of intracellular pS129 α-synuclein levels as determined by immunoblots performed at 15, 30, 50, 70 and 90 days of organoid maturation. Levels of pS129 α-synuclein are higher across all time points in 3xSNCA hMO. The data represents the summary of three independent hMO batches. Data is plotted by mutation (WT vs 3xSNCA). Statistical significance by Mann-Whitney U test: $^{**}p < 0.01$. Extensive description for how this graph was plotted is in materials and methods. (C) Representative images of 70-day old hMO stained with total α-synuclein (green), pS129 α-synuclein (red) and mature neuron marker MAP2 (white). 3xhMO show presence of aggregate-like structures rich in pS129 α-synuclein (inset). Scale bar = 50 μm. (D) Zoom in of inset in (C), showing aggregated pS129 α-synuclein and the presence of structures resembling Lewy neurites (white arrows). (E) Representative immunoblot of insoluble α-synuclein, which represents aggregated forms of the protein, at 50 days. Western blot is cropped from original images found in Supplementary original blots. (F) Quantification of insoluble α-synuclein at 50 days of organoid maturation showing the presence of more α-synuclein aggregates in the 3xSNCA organoids. Data is from 4 independent organoid batches. Each dot represents data from an individual Western blot run, where 12 organoids were pooled per line. Data presented as mean ± s.d. Statistical significance by Mann-Whitney U test: $^{**}p < 0.01$. (For interpretation of the references to color in this figure legend, the reader is referred to the web version of this article.)

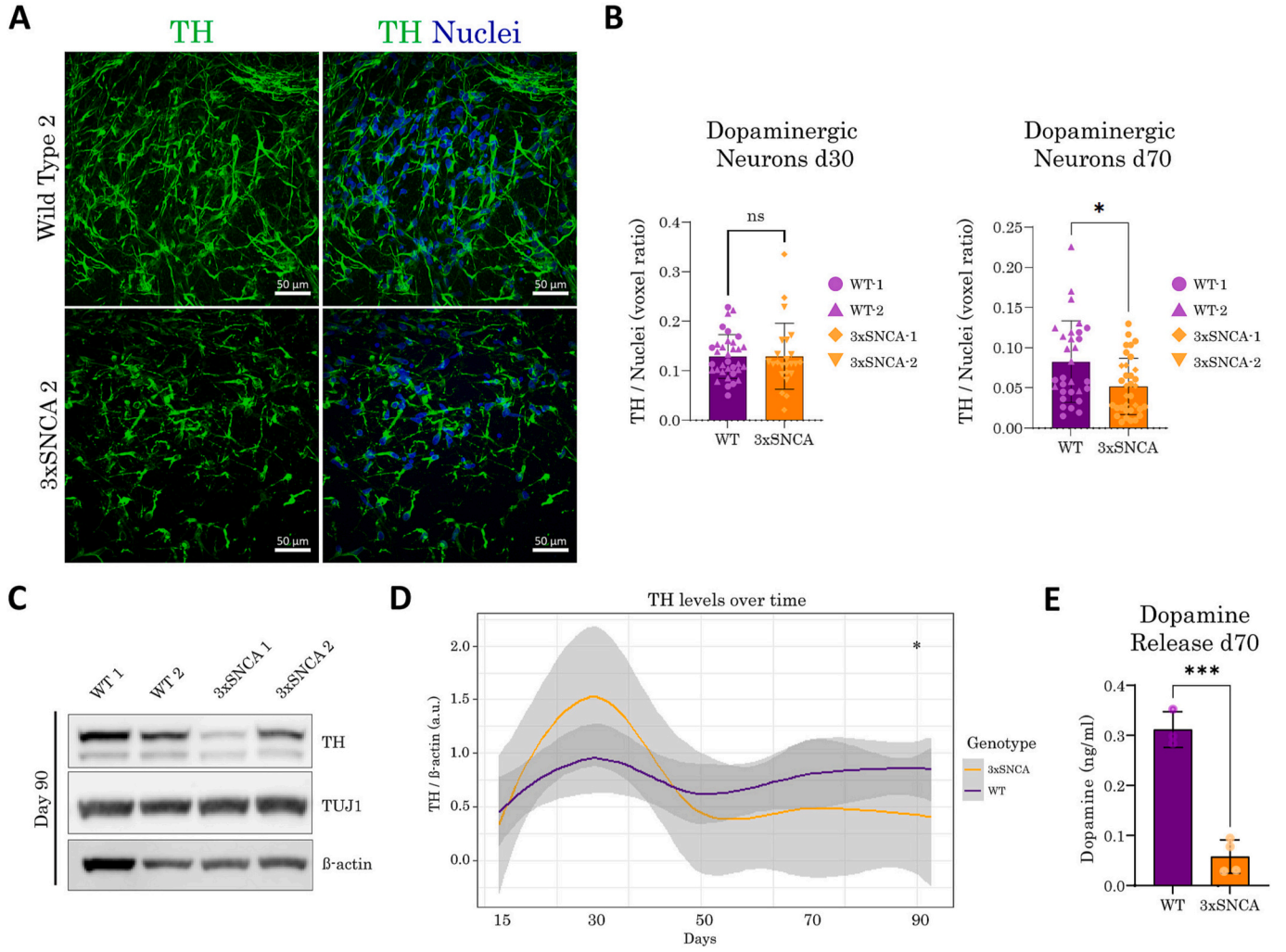

Fig. 4. Dopaminergic decline in 3xSNCA hMO. (A) Representative images of 70-day old hMO sections stained with TH (green) and Hoechst (blue) Scale bar = 50 μm. (B) Quantification of dopaminergic neuron levels at 30 and 70 days of organoid maturation. Data is from three independent organoid batches. Three to four organoids were analyzed per batch and three to six sections were analyzed per organoid. Each data point represents an individual organoid section. For 30 days: N(WT) = 35. N(3xSNCA) = 24. For 70 days: N(WT) = 30. N(3xSNCA) = 34. Data presented as mean ± s.d. Statistical significance by Mann-Whitney U test: $^{*}p < 0.05$. (C) Representative immunoblot of TH, TUJ1 and β-actin at 90 days of organoid maturation. Western blot is cropped from original images found in Supplementary original blots. (D) Time course of TH levels as determined by immunoblots performed at 15, 30, 50, 70 and 90 days of organoid maturation. The data represents the summary of three independent hMO batches. Data is plotted by mutation (WT vs 3xSNCA). Statistical significance by Mann-Whitney U test: $^{*}p < 0.05$. Extensive description for how this graph was plotted is in materials and methods. (E) 3xSNCA hMO release less dopamine at 70 days of organoid maturation as determined by dopamine ELISA. Each data point represents four independent hMO batches where media was pooled from the wells of three organoids. For this analysis only WT-1 and 3xSNCA-1 were used. N(WT) = 3. N(3xSNCA) = 4. Data presented as mean ± s.d. Statistical significance by Welch's t-test: $^{***}p < 0.001$. (For interpretation of the references to color in this figure legend, the reader is referred to the web version of this article.)

also associated with senescence, as it initiates the DNA damage response, which is a potent trigger for senescence (Kumari and Jat, 2021). We thus assessed the presence of phosphorylated H2AX (pH2AX), a prominent senescence associated heterochromatin foci (Fig. 5E). We found elevated levels of pH2AX foci in astrocyte nuclei in the 3xSNCA hMO (Fig. 5F). These findings are indicative of the increased presence of astrocytes in a senescent-like state in the patient specific hMO. Finally, to validate our findings, we performed qPCR for *CDNK2A*, which

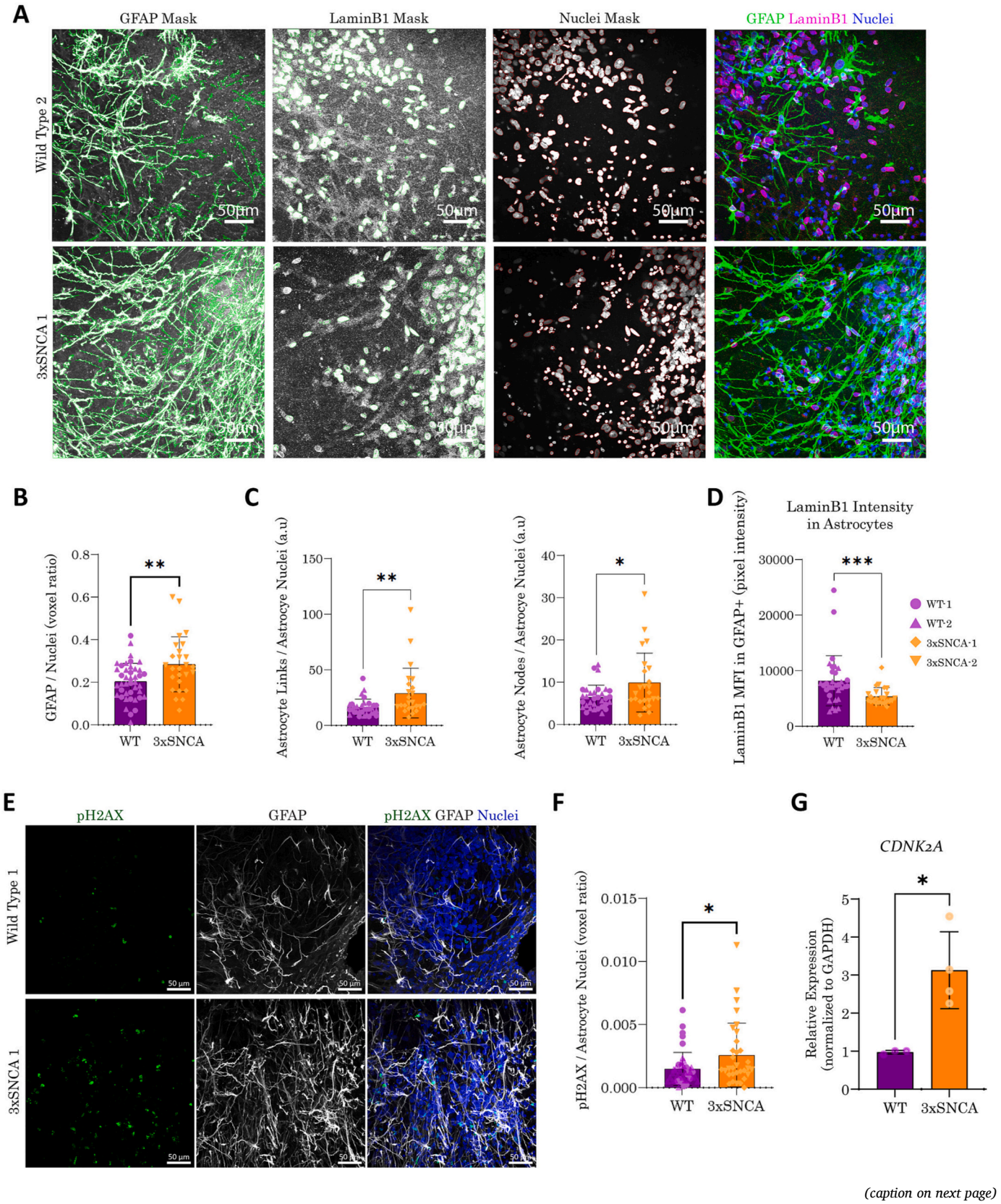

(caption on next page)

encodes p14 and p16. Both p14 and p16 are important tumor suppressors that mediate cell cycle control and inhibit cell proliferation. The upregulation of *CDNK2A* is a characteristic hallmark of senescence (Baker et al., 2008; He and Sharpless, 2017). In line with our other findings, *CDNK2A* was upregulated in the 3xSNCA hMO (Fig. 5G). We also evaluated whether neurons in our model displayed any signs of

Fig. 5. 3xSNCA hMO astrocytes show an increase in senescence associated hallmarks. (A) Representative images obtained from confocal imaging of 50-day old hMO sections at 40× magnification showing GFAP, lamin B1 and nuclei masks as identified by a Matlab image analysis script. Scale bar = 50 μm (B) 3xSNCA showed more GFAP+ astrocytes at 50 days. Data is from three independent organoid batches. Three to four organoids were analyzed per batch and three to six sections were analyzed per organoid. Each data point represents an individual organoid section. N(WT) = 32. N(3xSNCA) = 26. Data presented as mean ± s.d. Statistical significance by Mann-Whitney U test: $^{**}p < 0.01$. (C) Branching of astrocytes was assessed using a Matlab image analysis script that identifies the number of astrocyte links and nodes, normalized to the number of astrocytes (as determined by the number of nuclei in GFAP+ cells). 3xSNCA hMO astrocytes have significantly more links (left panel) and nodes (right panel), thus are more branched. Data is from three independent organoid batches. Three to four organoids were analyzed per batch and three to six sections were analyzed per organoid. Each data point represents an individual organoid section. N(WT) = 32. N(3xSNCA) = 24. Data presented as mean ± s.d. Statistical significance by Mann-Whitney U test: $^{*}p < 0.05$ and $^{**}p < 0.01$. (D) The expression of lamin B1 was significantly reduced in 3xSNCA hMO astrocytes at 50 days of organoid maturation. Data is from three independent organoid batches. Three to four organoids were analyzed per batch and three to six sections were analyzed per organoid. Each data point represents an individual organoid section. N(WT) = 33. N(3xSNCA) = 24. Data presented as mean ± s.d. Statistical significance by Mann-Whitney U test: $^{***}p < 0.001$. MFI – mean fluorescence intensity. (E) Representative immunostaining of pH2AX foci (green) in nuclei (blue) at 70 days. Scale bar = 10 μm. (F) There were significantly higher pH2AX foci present in 3xSNCA hMO astrocyte nuclei at 70 days of organoid maturation. Data is from four independent organoid batches. Three to four organoids were analyzed per batch and three to six sections were analyzed per organoid. Each data point represents an individual organoid section. N(WT) = 42. N(3xSNCA) = 32. Data presented as mean ± s.d. Statistical significance by Mann-Whitney U test: $^{*}p < 0.05$. (G) Real time PCR showed that *CDNK2A* which encodes p14/p16 is upregulated in 3xSNCA hMO at 90 days of organoid maturation. Data is from four independent organoid batches. Six organoids were pooled organoids per batch. Each data point represents qPCR data from one batch. Statistical significance by Welch's t-test: $^{*}p < 0.05$. (For interpretation of the references to color in this figure legend, the reader is referred to the web version of this article.)

senescence (Supplementary Fig. 5A). We found no differences in the level of MAP2+ mature neurons at 50 days of organoid maturation (Supplementary Fig. 5B). Interestingly, analysis of lamin B1 in MAP2+ neurons revealed significantly lower levels of the nuclear lamina protein in the 3xSNCA hMO (Supplementary Fig. 5C). However, assessment of pH2AX in non-astrocytic cells did not show any enrichment of heterochromatin foci (Supplementary Fig. 5D). As most of the non-astrocytic cells in the hMO are neurons at 50 days, this implies that the neuronal cells do not show accumulation of senescence associated DNA foci. Thus, our findings did not support a senescent-like phenotype in neurons. Altogether, our results suggest that astrocytes in the 3xSNCA hMO acquire a senescent-like phenotype, possibly due to the accumulation of pathological α-synuclein, which may have implications on PD etiology.

4. Discussion

The progressive degeneration of midbrain dopaminergic neurons and the presence of proteinaceous inclusions mainly comprising α-synuclein are the main neuropathological hallmarks of PD. Here, we describe a robust and reproducible patient-specific in vitro model system that is able to endogenously recapitulate these hallmarks, and allows for the study of the temporal molecular and cellular changes that underlie PD pathology and progression. Our 3xSNCA midbrain organoids showed significantly higher levels of intra and extracellular α-synuclein. They also displayed the presence of pS129 rich aggregate-like structures reminiscent of Lewy pathology. Our study supports other recently published work in midbrain organoids with PD related mutations in *SNCA*, showing the recapitulation of PD related phenotypes (Jo et al., 2021; Mohamed et al., 2021). Moreover, we found an association between the accumulation of pathogenic α-synuclein and the acquisition of a senescent-like phenotype in astrocytes in our patient-specific hMO.

Our study followed a time course of dopaminergic neuron development in the organoids, which allowed us to assess dynamics that may have implications in disease pathogenesis. We found a decline in dopaminergic neurons in the 3xSNCA hMO at 70 days which corresponded with the progressive decline of TH enzyme levels which began after 50 days and was most significant after 90 days. Moreover, dopamine production was drastically reduced in the 3xSNCA hMO, indicative of reduced functionality of the dopaminergic neurons. Taken together, these findings support the recapitulation of dopaminergic neuron loss in a progressive manner in 3xSNCA organoids.

Astrocytes in the 3xSNCA hMO showed nuclear lamina defects and increased presence of the senescence associated heterochromatin foci pH2AX. We also found an overall upregulation of *CDNK2A,* a gene associated with cell cycle regulation, in the 3xSNCA hMO. These findings suggest that astrocytes from the patient-specific organoids acquire a senescent-like phenotype. On the other hand, while we did observe nuclear lamina deficits in the neurons, this was not accompanied by increased senescence associated heterochromatic foci. Therefore, the acquisition of the senescence-like phenotype appears to be more prominent in astrocytes than in neurons at this time point. The acquisition of the senescence-like phenotype in the astrocytes, which was observed at 50 days, preceded the loss of dopaminergic neurons, which was most significant at 70 days. Therefore, we speculate that the presence of senescent astrocytes may have a detrimental impact on the dopaminergic neurons in the 3xSNCA hMO. To further validate the senescent phenotype, a future experiment employing the senescence-associated β-galactosidase (SA-β-gal) assay would be useful. SA-β-gal is an inducible lysosomal enzyme abundantly produced in senescent cells. Previous research has shown that overexpression of α-synuclein in SH-SY5Y cells increases SA-β-gal levels (Yoon et al., 2022). The SA-β-gal assay has proven effective in exploring senescence-related changes in human cortical brain organoids (Shaker et al., 2021), therefore incorporating this assay could provide valuable insights into the senescent status of the astrocytes within the 3xSNCA hMO.

Astrosenescence has recently gained attention as the loss of astrocytic function and gain of a proinflammatory phenotype due to senescence is thought to have significant implications for neurodegenerative diseases (Cohen and Torres, 2019; Lazic et al., 2022). In addition, several studies have shown that the interaction between healthy neurons and senescent astrocytes impairs neuronal function, synaptic plasticity, synaptic vesicle size and synapse maturation (Limbad et al., 2020; Bussian et al., 2018). These effects are thought to be mediated through the senescence associated secretory phenotype (SASP) (Kritsilis et al., 2018), which is the release of proinflammatory mediators, reactive oxygen species and metalloproteinases by senescent cells. Thus, one could speculate that the presence of senescent astrocytes in the 3xSNCA hMO may negatively impact the dopaminergic neurons via the effects of the SASP. We also found an increase in the number of GFAP+ astrocytes in the 3xSNCA hMO at 50 days, which may be indicative of astrogliosis. Mild to moderate astrogliosis is associated with the upregulation of GFAP (Sofroniew, 2014). While astrosenescence and astrogliosis are two distinct astrocytic states, they are both initiated by cytotoxic injury (Cohen and Torres, 2019). Therefore, there is a high likelihood that we have a diverse set of astrocytes in the organoids reflecting different cellular states like reactivity and senescence. Recently, cellular senescence has been identified as a contributor to neurodegenerative disease as senescent cells accumulate in the context of neurodegenerative diseases like PD, Alzheimer's, multiple sclerosis and amyotrophic lateral sclerosis (Si et al., 2021).

There is mounting evidence that pathological α-synuclein may be a driver of cellular senescence. As the 3xSNCA hMO showed accumulation of α-synuclein and its phosphorylated form, we propose that the pathological α-synuclein may contribute to the observed astrosenescence

phenotype. Verma et al. showed that α-synuclein pre-formed fibrils (PFFs) can induce senescence in cell lines and mouse models (Verma et al., 2021). In their study, PFFs triggered senescence in primary astrocytes and microglia, and to a lesser extent in primary cortical neurons. These findings support the idea that glial cells may be particularly vulnerable to pathological α-synuclein induced senescence. This is in line with our findings where we observed a senescent phenotype in the astrocytes but not in the neurons at 50 days. Interestingly, they also found increased GFAP expression in adult mouse midbrains and striatum following injection with PFFs (Verma et al., 2021), which is also consistent with our results. Our results are further supported by findings from Di Marco Vieira et al., who demonstrated that extracellular α-synuclein induces astrocyte activation, resulting in the upregulation of a secretory phenotype in a human astroglia cell line (Di Marco et al., 2020). Recently, another study demonstrated that overexpression of α-synuclein in human neuroblastoma cells has been shown to activate the p53 pathway and DNA damage responses, and induce cellular senescence (Yoon et al., 2022). Moreover, they found that α-synuclein transgenic mice displayed increased pS129 α-synuclein along with increased presence of DSBs and senescence associated markers at early, presymptomatic stages of disease before dopaminergic neuron loss. This also supports the hypothesis that cellular senescence may be a pathogenic mechanism preceding dopaminergic degeneration. Besides its abundant expression at pre-synaptic terminals, α-synuclein has been shown to be expressed in the nucleus (Koss et al., 2022; Goers et al., 2003). A potential nuclear function of α-synuclein that has been recently proposed is that under physiological conditions, it is a DNA binding protein that modulates DNA repair. It was postulated that the cytoplasmic aggregation of α-synuclein reduces its nuclear levels, thus reducing the DNA repair capacity of cells and increasing the presence of double strand breaks (Schaser et al., 2019). As DNA damage is a potent inducer of senescence in cells, we speculate that the senescent-like phenotypes we observed in the 3xSNCA hMO may at least in part be explained by this phenomenon. To validate this, it would be important to study the localization of α-synuclein in the nucleus and whether this is altered with aggregation in our model.

As senescence is often associated with aging, it may be surprising that we observed senescence in our organoid model, which is more reflective of the brain during neurodevelopment. However, while senescence is often associated with aging, there has been a growing body of work describing other mechanisms through which senescence can be induced, independently of aging. For example, DNA-damage-induced senescence and stress-induced senescence are mechanisms that have been implicated in diseases like cancer (Muñoz-Espín and Serrano, 2014). Stress-induced senescence can be triggered by reactive oxygen species. Pathological α-synuclein has been implicated in increasing ROS levels (Puspita et al., 2017), and thus this could represent a potential mechanism in which senescence could be induced in our model.

Our findings, which highlight a potential role of senescence in PD pathogenesis, opens opportunities for the use of senolytics as a therapeutic strategy in the disease. Senolytics selectively kill senescent cells by targeting anti-apoptotic pathways that are upregulated during senescence. Notably, several senolytics have shown efficacy in improving cognition and lifespan in mouse models of neurodegeneration (Zhang et al., 2019; Musi et al., 2018; Riessland et al., 2019). In a recent study, Aguado and colleagues used senolytics, including Navitoclax, ABT-737 and a combination of Dasatinib and Quercetin, to prevent virus-induced cellular senescence in distinct neuronal populations in brain organoids (Aguado et al., 2023). This underscores the potential of senolytic drugs in mitigating senescence-related effects in neural tissues. Therefore, our midbrain organoid model emerges as an ideal platform for future experiments evaluating the effectiveness of diverse senolytic drugs in preventing cellular senescence and associated pathology in Parkinson's disease.

Altogether, our results suggest that elevated α-synuclein is associated to the acquisition of a senescent-like phenotype in astrocytes, preceding dopaminergic degeneration. This may have implications on PD pathogenesis as astrosenescence may promote the vulnerability of dopaminergic neurons. While further research is required to elucidate the underlying mechanisms, our hMO model's ability to recapitulate these phenotypes will allow us to further explore this aspect of PD pathogenesis and test relevant therapeutic strategies.

Funding

The work leading to this manuscript was supported through funding to JCS's lab: Fonds National de la Recherche Luxembourg (PRIDE17/12244779/PARK-QC; CORE C21/DM/15839823; BRIDGES18/BM/12719664_MOTASYN; INTER/FWF/19/14117540/PDage). The U.S. Army Medical Research and Materiel Command endorsed by the U.S. Army through the Parkinson's Research Program Investigator-Initiated Research Award under Award No. W81XWH-17-PRP-IIRA. Opinions, interpretations, conclusions, and recommendations are those of the author and are not necessarily endorsed by the U.S. Army. SB received funding from the Fonds National de la Recherche Luxembourg (Core C21/DM/15839823).

CRediT authorship contribution statement

Mudiwa N. Muwanigwa: Data curation, Formal analysis, Investigation, Methodology, Writing – original draft, Writing – review & editing. **Jennifer Modamio-Chamarro:** Data curation, Formal analysis, Investigation, Methodology, Writing – review & editing. **Paul M.A. Antony:** Formal analysis, Visualization, Writing – review & editing. **Gemma Gomez-Giro:** Data curation, Methodology, Writing – review & editing. **Rejko Krüger:** Project administration, Supervision, Writing – review & editing. **Silvia Bolognin:** Formal analysis, Supervision, Writing – review & editing, Data curation. **Jens C. Schwamborn:** Conceptualization, Data curation, Funding acquisition, Investigation, Project administration, Writing – original draft, Writing – review & editing.

Declaration of competing interest

SB and JCS are cofounders and shareholders of OrganoTherapeutics société à responsabilité limitée simplifiée (SARL-S).

Data availability

All original and processed data as well as scripts that support the findings of this study are publicly available at: doi:10.17881/zmmj-8z40.

Acknowledgements

We thank Professor Tilo Kunath, Coriell Institute, GIBCO and EBiSC for providing iPSC lines for this study. Microscopy work was supported by the LCSB Bioimaging Platform. We also thank the private donors who support our work at the Luxembourg Center for Systems Biomedicine.

Appendix A. Supplementary data

Supplementary data to this article can be found online at https://doi.org/10.1016/j.mcn.2024.103919.

References

Aguado, J., Amarilla, A.A., Taherian, Fard A., et al., 2023. Senolytic therapy alleviates physiological human brain aging and COVID-19 neuropathology. Nat Aging. 3 https://doi.org/10.1038/s43587-023-00519-6.

Ahfeldt T, Ordureau A, Bell C, et al. Pathogenic pathways in early-onset autosomal recessive Parkinson's disease discovered using isogenic human dopaminergic neurons. Stem Cell Reports. Jan 14 2020;14(1):75–90. doi:https://doi.org/10.1016/j.stemcr.2019.12.005.

Anderson, J.P., Walker, D.E., Goldstein, J.M., et al., 2006. Phosphorylation of Ser-129 is the dominant pathological modification of alpha-synuclein in familial and sporadic Lewy body disease. J. Biol. Chem. 281 (40), 29739–29752. https://doi.org/10.1074/jbc.M600933200 (Oct 6).

Appel-Cresswell, S., Vilarino-Guell, C., Encarnacion, M., et al., 2013. Alpha-synuclein p.H50Q, a novel pathogenic mutation for Parkinson's disease. Mov. Disord. 28 (6), 811–813. https://doi.org/10.1002/mds.25421 (Jun).

Baker, D.J., Jin, F., van Deursen, J.M., 2008. The yin and yang of the Cdkn2a locus in senescence and aging. Cell Cycle 7 (18), 2795–2802. https://doi.org/10.4161/cc.7.18.6687 (Sep 15).

Bobela, W., Aebischer, P., Schneider, B.L., 2015. Alpha-synuclein as a mediator in the interplay between aging and Parkinson's disease. Biomolecules 5 (4), 2675–2700.

Bolognin, S., Fossépré, M., Qing, X., et al., 2019. 3D cultures of Parkinson's disease-specific dopaminergic neurons for high content phenotyping and drug testing. Adv Sci (Weinh). 6 (1), 1800927 https://doi.org/10.1002/advs.201800927 (Jan 9).

Burré, J., Sharma, M., Tsetsenis, T., Buchman, V., Etherton, M.R., Südhof, T.C., 2010. Alpha-synuclein promotes SNARE-complex assembly in vivo and in vitro. Science 329 (5999), 1663–1667. https://doi.org/10.1126/science.1195227 (Sept 24).

Bussian, T.J., Aziz, A., Meyer, C.F., Swenson, B.L., van Deursen, J.M., Baker, D.J., 2018. Clearance of senescent glial cells prevents tau-dependent pathology and cognitive decline. Nature 562 (7728), 578–582. https://doi.org/10.1038/s41586-018-0543-y (Oct).

Butin-Israeli, V., Adam, S.A., Jain, N., et al., 2015. Role of lamin B1 in chromatin instability. Mol. Cell. Biol. 35 (5), 884–898. https://doi.org/10.1128/MCB.01145-14.

Camps J, Erdos MR, Ried T. The role of lamin B1 for the maintenance of nuclear structure and function. Nucleus 2015/01/02 2015;6(1):8–14. doi:https://doi.org/10.1080/19491034.2014.1003510.

Chen, V., Moncalvo, M., Tringali, D., et al., 2020. The mechanistic role of alpha-synuclein in the nucleus: impaired nuclear function caused by familial Parkinson's disease SNCA mutations. Hum. Mol. Genet. 29 (18), 3107–3121. https://doi.org/10.1093/hmg/ddaa183 (Nov 4).

Chinta, S.J., Woods, G., Demaria, M., et al., 2018. Cellular senescence is induced by the environmental neurotoxin paraquat and contributes to neuropathology linked to Parkinson's disease. Cell Rep. 22 (4), 930–940. https://doi.org/10.1016/j.celrep.2017.12.092 (Jan 23).

Choi, M.G., Kim, M.J., Kim, D.G., Yu, R., Jang, Y.N., Oh, W.J., 2018. Sequestration of synaptic proteins by alpha-synuclein aggregates leading to neurotoxicity is inhibited by small peptide. PLoS One 13 (4), e0195339. https://doi.org/10.1371/journal.pone.0195339.

Cohen, J., Torres, C., 2019. Astrocyte senescence: evidence and significance. Aging Cell 18 (3), e12937. https://doi.org/10.1111/acel.12937.

Di Marco, Vieira B., et al., 2020. Extracellular alpha-synuclein promotes a neuroinhibitory secretory phenotype in astrocytes. Life 10 (9), 183. https://doi.org/10.3390/life100901.

Eliezer, D., Kutluay, E., Bussell Jr., R., Browne, G., 2001. Conformational properties of alpha-synuclein in its free and lipid-associated states. J. Mol. Biol. 307 (4), 1061–1073. https://doi.org/10.1006/jmbi.2001.4538 (Apr 6).

Fortin, D.L., Nemani, V.M., Voglmaier, S.M., Anthony, M.D., Ryan, T.A., Edwards, R.H., 2005. Neural activity controls the synaptic accumulation of alpha-synuclein. J. Neurosci. 25 (47), 10913–10921. https://doi.org/10.1523/jneurosci.2922-05.2005 (Nov 23).

Freund, A., Laberge, R.M., Demaria, M., Campisi, J., 2012. Lamin B1 loss is a senescence-associated biomarker. Mol. Biol. Cell 23 (11), 2066–2075. https://doi.org/10.1091/mbc.E11-10-0884 (Jun).

Fujioka, S., Ogaki, K., Tacik, P.M., Uitti, R.J., Ross, O.A., Wszolek, Z.K., 2014. Update on novel familial forms of Parkinson's disease and multiple system atrophy. Parkinsonism Relat. Disord. 20 (Suppl. 1), S29–S34. https://doi.org/10.1016/s1353-8020(13)70010-5 (Jan).

Galet B, Cheval H, Ravassard P. Patient-derived midbrain organoids to explore the molecular basis of Parkinson's disease. Review. Frontiers in Neurology. 2020-September-04 2020;11doi:https://doi.org/10.3389/fneur.2020.01005.

Geertsma, H.M., Suk, T.R., Ricke, K.M., et al., 2022. Constitutive nuclear accumulation of endogenous alpha-synuclein in mice causes motor impairment and cortical dysfunction, independent of protein aggregation. Hum. Mol. Genet. 31 (21), 3613–3628. https://doi.org/10.1093/hmg/ddac035.

Goers, J., Manning-Bog, A.B., McCormack, A.L., et al., 2003. Nuclear localization of alpha-synuclein and its interaction with histones. Biochemistry 42 (28), 8465–8471. https://doi.org/10.1021/bi0341152 (Jul 22).

Gomez-Giro, G., Arias-Fuenzalida, J., Jarazo, J., et al., 2019. Synapse alterations precede neuronal damage and storage pathology in a human cerebral organoid model of CLN3-juvenile neuronal ceroid lipofuscinosis. Acta Neuropathol. Commun. 7 (1), 222. https://doi.org/10.1186/s40478-019-0871-7 (Dec 30).

He, S., Sharpless, N.E., 2017. Senescence in health and disease. Cell 169 (6), 1000–1011. https://doi.org/10.1016/j.cell.2017.05.015 (Jun 1).

Hernandez-Segura, A., Nehme, J., Demaria, M., 2018. Hallmarks of cellular senescence. Trends Cell Biol. 28 (6), 436–453. https://doi.org/10.1016/j.tcb.2018.02.001 (Jun).

Hoffman-Zacharska, D., Koziorowski, D., Ross, O.A., et al., 2013. Novel A18T and pA29S substitutions in α-synuclein may be associated with sporadic Parkinson's disease. Parkinsonism Relat. Disord. 19 (11), 1057–1060. https://doi.org/10.1016/j.parkreldis.2013.07.011 (Nov).

Jarazo, J., Barmpa, K., Modamio, J., et al., 2022. Parkinson's disease phenotypes in patient neuronal cultures and brain organoids improved by 2-hydroxypropyl-β-cyclodextrin treatment. Mov. Disord. 37 (1), 80–94. https://doi.org/10.1002/mds.28810 (Jan).

Jin, H., Kanthasamy, A., Ghosh, A., Yang, Y., Anantharam, V., Kanthasamy, A.G., 2011. α-Synuclein negatively regulates protein kinase Cδ expression to suppress apoptosis in dopaminergic neurons by reducing p300 histone acetyltransferase activity. J. Neurosci. 31 (6), 2035–2051. https://doi.org/10.1523/jneurosci.5634-10.2011 (Feb 9).

Jo, J., Xiao, Y., Sun, A.X., et al., 2016. Midbrain-like organoids from human pluripotent stem cells contain functional dopaminergic and neuromelanin-producing neurons. Cell Stem Cell 19 (2), 248–257. https://doi.org/10.1016/j.stem.2016.07.005 (Aug 4).

Jo, J., Yang, L., Tran, H.D., et al., 2021. Lewy body-like inclusions in human midbrain organoids carrying glucocerebrosidase and α-synuclein mutations. Ann. Neurol. 90 (3), 490–505. https://doi.org/10.1002/ana.26166 (Sep).

Kiely, A.P., Asi, Y.T., Kara, E., et al., 2013. α-Synucleinopathy associated with G51D SNCA mutation: a link between Parkinson's disease and multiple system atrophy? Acta Neuropathol. 125 (5), 753–769. https://doi.org/10.1007/s00401-013-1096-7 (May).

Kim, H., Park, H.J., Choi, H., et al., 2019. Modeling G2019S-LRRK2 sporadic Parkinson's disease in 3D midbrain organoids. Stem Cell Reports 12 (3), 518–531. https://doi.org/10.1016/j.stemcr.2019.01.020 (Mar 5).

Koss, D.J., Erskine, D., Porter, A., et al., 2022. Nuclear alpha-synuclein is present in the human brain and is modified in dementia with Lewy bodies. Acta Neuropathologica Communications 10 (1), 98. https://doi.org/10.1186/s40478-022-01403-x (2022/07/06).

Kritsilis, M., S, V.R., Koutsoudaki, P.N., Evangelou, K., Gorgoulis, V.G., Papadopoulos, D., 2018. Ageing, cellular senescence and neurodegenerative disease. Int. J. Mol. Sci. 19 (10) https://doi.org/10.3390/ijms19102937 (Sep 27).

Krüger, R., Kuhn, W., Müller, T., et al., 1998. Ala30Pro mutation in the gene encoding alpha-synuclein in Parkinson's disease. Nat. Genet. 18 (2), 106–108. https://doi.org/10.1038/ng0298-106 (Feb).

Kumari R, Jat P. Mechanisms of cellular senescence: cell cycle arrest and senescence associated secretory phenotype. Review. Frontiers in Cell and Developmental Biology. 2021-March-29 2021;9doi:https://doi.org/10.3389/fcell.2021.645593.

Lashuel, H.A., Petre, B.M., Wall, J., et al., 2002. Alpha-synuclein, especially the Parkinson's disease-associated mutants, forms pore-like annular and tubular protofibrils. J. Mol. Biol. 322 (5), 1089–1102. https://doi.org/10.1016/s0022-2836(02)00735-0 (Oct 4).

Lazic, A., Balint, V., Stanisavljevic Ninkovic, D., Peric, M., Stevanovic, M., 2022. Reactive and senescent astroglial phenotypes as hallmarks of brain pathologies. Int. J. Mol. Sci. 23 (9) https://doi.org/10.3390/ijms23094995 (Apr 30).

Li, W., Lee, M.K., 2005. Antiapoptotic property of human alpha-synuclein in neuronal cell lines is associated with the inhibition of caspase-3 but not caspase-9 activity. J. Neurochem. 93 (6), 1542–1550. https://doi.org/10.1111/j.1471-4159.2005.03146.x (Jun).

Limbad, C., Oron, T.R., Alimirah, F., et al., 2020. Astrocyte senescence promotes glutamate toxicity in cortical neurons. PLoS One 15 (1), e0227887. https://doi.org/10.1371/journal.pone.0227887.

Malkus KA, Tsika E, Ischiropoulos H. Oxidative modifications, mitochondrial dysfunction, and impaired protein degradation in Parkinson's disease: how neurons are lost in the Bermuda triangle. Mol. Neurodegener. 2009/06/05 2009;4(1):24. doi:https://doi.org/10.1186/1750-1326-4-24.

Martínez-Cué, C., Rueda, N., 2020. Cellular senescence in neurodegenerative diseases. Front. Cell. Neurosci. 14, 16. https://doi.org/10.3389/fncel.2020.00016.

Matias, I., Diniz, L.P., Damico, I.V., et al., 2022. Loss of lamin-B1 and defective nuclear morphology are hallmarks of astrocyte senescence in vitro and in the aging human hippocampus. Aging Cell 21 (1), e13521. https://doi.org/10.1111/acel.13521.

Miller, D.W., Hague, S.M., Clarimon, J., et al., 2004. Alpha-synuclein in blood and brain from familial Parkinson disease with SNCA locus triplication. Neurology 62 (10), 1835–1838. https://doi.org/10.1212/01.wnl.0000127517.33208.f4 (May 25).

Mohamed, N.-V., Sirois, J., Ramamurthy, J., et al., 2021. Midbrain organoids with an SNCA gene triplication model key features of synucleinopathy. Brain Communications 3 (4). https://doi.org/10.1093/braincomms/fcab223.

Monzel, A.S., Smits, L.M., Hemmer, K., et al., 2017. Derivation of human midbrain-specific organoids from neuroepithelial stem cells. Stem Cell Rep. 8 (5), 1144–1154. https://doi.org/10.1016/j.stemcr.2017.03.010 (May 9).

Monzel, A.S., Hemmer, K., Kaoma, T., et al., 2020. Machine learning-assisted neurotoxicity prediction in human midbrain organoids. Parkinsonism Relat. Disord. 75, 105–109. https://doi.org/10.1016/j.parkreldis.2020.05.011 (Jun).

Muñoz-Espín D, Serrano M. Cellular senescence: from physiology to pathology. Nat. Rev. Mol. Cell Biol. 2014/07/01 2014;15(7):482–496. doi:https://doi.org/10.1038/nrm3823.

Musi, N., Valentine, J.M., Sickora, K.R., et al., 2018. Tau protein aggregation is associated with cellular senescence in the brain. Aging Cell 17 (6), e12840. https://doi.org/10.1111/acel.12840 (Dec).

Nickels SL, Modamio J, Mendes-Pinheiro B, Monzel AS, Betsou F, Schwamborn JC. Reproducible generation of human midbrain organoids for in vitro modeling of Parkinson's disease. Stem Cell Res. 2020/07/01/ 2020;46:101870. doi:https://doi.org/10.1016/j.scr.2020.101870.

Pasanen, P., Myllykangas, L., Siitonen, M., et al., 2014. Novel α-synuclein mutation A53E associated with atypical multiple system atrophy and Parkinson's disease-type pathology. Neurobiol. Aging 35 (9), 2180.e1–2180.e5. https://doi.org/10.1016/j.neurobiolaging.2014.03.024 (Sep).

Polymeropoulos, M.H., Lavedan, C., Leroy, E., et al., 1997. Mutation in the alpha-synuclein gene identified in families with Parkinson's disease. Science 276 (5321), 2045–2047. https://doi.org/10.1126/science.276.5321.2045 (Jun 27).

Potashkin, J.A., Blume, S.R., Runkle, N.K., 2010. Limitations of animal models of Parkinson's disease. Parkinsons Dis. 2011, 658083 https://doi.org/10.4061/2011/658083 (Dec 20).

Puspita, L., Chung, S.Y., Shim, J.W., 2017. Oxidative stress and cellular pathologies in Parkinson's disease. Mol Brain. 10 (1), 53. https://doi.org/10.1186/s13041-017-0340-9 (Nov 28).

Reinhardt, P., Glatza, M., Hemmer, K., et al., 2013. Derivation and expansion using only small molecules of human neural progenitors for neurodegenerative disease modeling. PLoS One 8 (3), e59252. https://doi.org/10.1371/journal.pone.0059252.

Riessland, M., Kolisnyk, B., Kim, T.W., et al., 2019. Loss of SATB1 induces p21-dependent cellular senescence in post-mitotic dopaminergic neurons. Cell Stem Cell 25 (4), 514–530.e8. https://doi.org/10.1016/j.stem.2019.08.013 (Oct 3).

Schaser AJ, Osterberg VR, Dent SE, et al. Alpha-synuclein is a DNA binding protein that modulates DNA repair with implications for Lewy body disorders. Sci. Rep. 2019/07/29 2019;9(1):10919. doi:https://doi.org/10.1038/s41598-019-47227-z.

Shaker, M.R., Aguado, J., Chaggar, H.K., Wolvetandg, E.J., 2021. Klotho inhibits senescence in human brain organoids. npj Aging and Mechanisms of Disease. 7 (18) https://doi.org/10.1038/s41514-021-00070-x.

Si Z, Sun L, Wang X. Evidence and perspectives of cell senescence in neurodegenerative diseases. Biomed. Pharmacother. 2021/05/01/ 2021;137:111327. doi:https://doi.org/10.1016/j.biopha.2021.111327.

Sikora, E., Bielak-Zmijewska, A., Dudkowska, M., et al., 2021. Cellular senescence in brain aging. Front. Aging Neurosci. 13, 646924 https://doi.org/10.3389/fnagi.2021.646924.

Singleton, A.B., Farrer, M., Johnson, J., et al., 2003. Alpha-synuclein locus triplication causes Parkinson's disease. Science 302 (5646), 841. https://doi.org/10.1126/science.1090278 (Oct 31).

Smits LM, Schwamborn JC. Midbrain organoids: a new tool to investigate Parkinson's disease. Review. Frontiers in Cell and Developmental Biology. 2020-May-19 2020;8doi:https://doi.org/10.3389/fcell.2020.00359.

Smits LM, Reinhardt L, Reinhardt P, et al. Modeling Parkinson's disease in midbrain-like organoids. npj Parkinson's Disease. 2019/04/05 2019;5(1):5. doi:https://doi.org/10.1038/s41531-019-0078-4.

Sofroniew, M.V., 2014. Astrogliosis. Cold Spring Harb. Perspect. Biol. 7 (2), a020420 https://doi.org/10.1101/cshperspect.a020420 (Nov 7).

Spillantini, M.G., Schmidt, M.L., Lee, V.M., Trojanowski, J.Q., Jakes, R., Goedert, M., 1997. Alpha-synuclein in Lewy bodies. Nature 388 (6645), 839–840. https://doi.org/10.1038/42166 (Aug 28).

Ulmer, T.S., Bax, A., 2005. Comparison of structure and dynamics of micelle-bound human alpha-synuclein and Parkinson disease variants. J. Biol. Chem. 280 (52), 43179–43187. https://doi.org/10.1074/jbc.M507624200 (Dec 30).

Verma, D.K., Seo, B.A., Ghosh, A., et al., 2021. Alpha-synuclein preformed fibrils induce cellular senescence in Parkinson's disease models. Cells 10 (7). https://doi.org/10.3390/cells10071694 (Jul 5).

Volpicelli-Daley, L.A., Luk, K.C., Patel, T.P., et al., 2011. Exogenous α-synuclein fibrils induce Lewy body pathology leading to synaptic dysfunction and neuron death. Neuron 72 (1), 57–71. https://doi.org/10.1016/j.neuron.2011.08.033 (Oct 6).

Waudby, C.A., Camilloni, C., Fitzpatrick, A.W.P., et al., 2013. In-cell NMR characterization of the secondary structure populations of a disordered conformation of α-synuclein within E. coli cells. PLoS One 8 (8), e72286. https://doi.org/10.1371/journal.pone.0072286.

Weinreb, P.H., Zhen, W., Poon, A.W., Conway, K.A., Lansbury Jr., P.T., 1996. NACP, a protein implicated in Alzheimer's disease and learning, is natively unfolded. Biochemistry 35 (43), 13709–13715. https://doi.org/10.1021/bi961799n (Oct 29).

Yoon Y-S, You JS, Kim T-K, et al. Senescence and impaired DNA damage responses in alpha-synucleinopathy models. Exp. Mol. Med. 2022/02/01 2022;54(2):115–128. doi:https://doi.org/10.1038/s12276-022-00727-x.

Zagare, A., Gobin, M., Monzel, A.S., Schwamborn, J.C., 2021. A robust protocol for the generation of human midbrain organoids. STAR Protoc. 2 (2), 100524 https://doi.org/10.1016/j.xpro.2021.100524 (Jun 18).

Zarranz, J.J., Alegre, J., Gómez-Esteban, J.C., et al., 2004. The new mutation, E46K, of alpha-synuclein causes Parkinson and Lewy body dementia. Ann. Neurol. 55 (2), 164–173. https://doi.org/10.1002/ana.10795 (Feb).

Zhang, P., Kishimoto, Y., Grammatikakis, I., et al., 2019. Senolytic therapy alleviates Aβ-associated oligodendrocyte progenitor cell senescence and cognitive deficits in an Alzheimer's disease model. Nat. Neurosci. 22 (5), 719–728. https://doi.org/10.1038/s41593-019-0372-9 (May).